# Subduction of the Nazca Ridge and the Inca Plateau: Insights into the formation of ore deposits in Peru

Gideon Rosenbaum [a],[*], David Giles [b], Mark Saxon [c], Peter G. Betts [b], Roberto F. Weinberg [b], Cecile Duboz [b]

[a] *Institut für Geowissenschaften, Johannes Gutenberg Universität, Mainz 55128, Germany*
[b] *Australian Crustal Research Centre, School of Geosciences, Monash University, Melbourne 3800, Victoria, Australia*
[c] *Sierra Minerals Ltd, PO Box 2213, Bendigo DC 3554, Victoria, Australia*

## Abstract

A large number of ore deposits that formed in the Peruvian Andes during the Miocene (15–5 Ma) are related to the subduction of the Nazca plate beneath the South American plate. Here we show that the spatial and temporal distribution of these deposits correspond with the arrival of relatively buoyant topographic anomalies, namely the Nazca Ridge in central Peru and the now-consumed Inca Plateau in northern Peru, at the subduction zone. Plate reconstruction shows a rapid metallogenic response to the arrival of the topographic anomalies at the subduction trench. This is indicated by clusters of ore deposits situated within the proximity of the laterally migrating zones of ridge subduction. It is accordingly suggested that tectonic changes associated with impingement of the aseismic ridge into the subduction zone may trigger the formation of ore deposits in metallogenically fertile suprasubduction environments.
© 2005 Elsevier B.V. All rights reserved.

*Keywords:* Nazca Ridge; ore deposits; subduction; Peru; plate reconstruction

## 1. Introduction

Magmatic–hydrothermal ore deposits in suprasubduction environments (i.e. crust above a subduction zone) are one of the major sources for the world's copper and gold. These deposits are particularly abundant in the Andes (Fig. 1), where they are associated with subduction-related magmatic arcs. Eastward subduction of oceanic lithosphere (the Nazca plate) beneath the continental South American plate has been progressively taking place for the last ~200 Ma. Nevertheless, the spatial and temporal distribution of ore deposits throughout the Andes
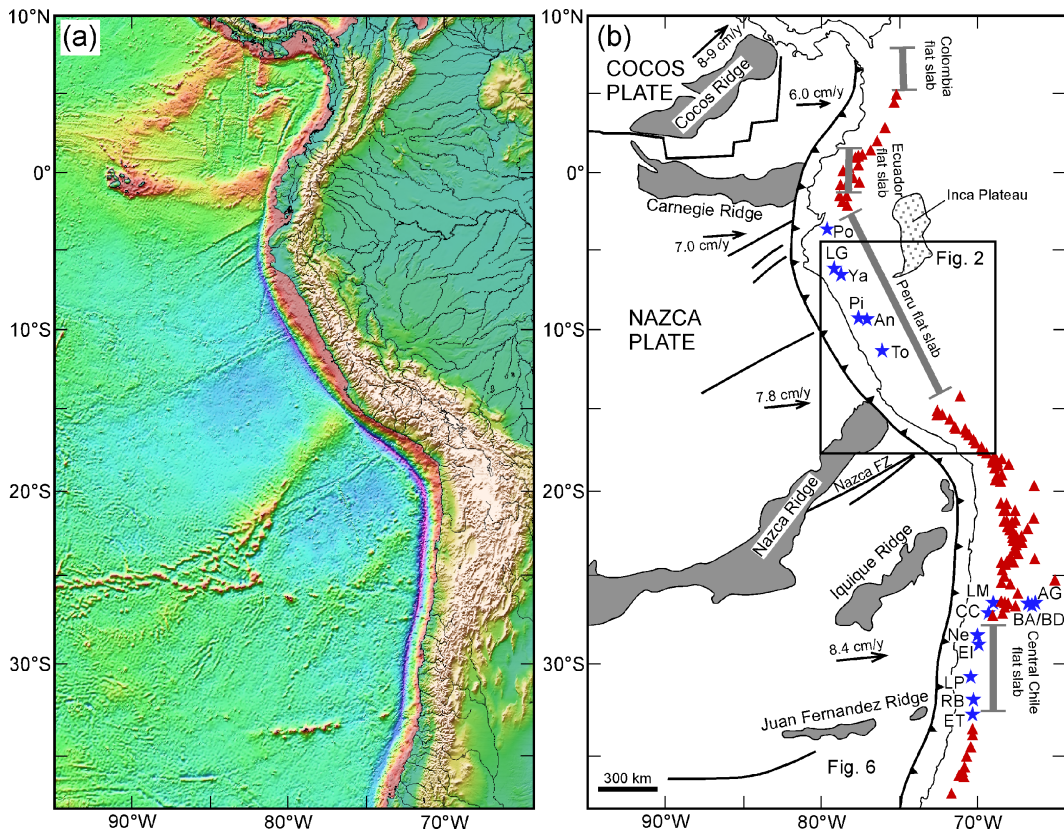
Fig. 1. (a) Topographic image of the eastern Pacific Ocean and the South American Andes (after [53]). (b) Main tectonic features (modified after [9,24]), with topographic anomalies (grey areas) and the postulated location of the consumed Inca Plateau (dotted area). Black triangles indicate subduction zone, blue stars indicate locations of the largest young (<18 Ma) Cu and Au deposits in the Andes (see Tables 2 and 3), and red triangles indicate active volcanoes. Present-day plate velocities are indicated by arrows (after [54]). Also shown are flat slab segments within the subduction zone (thick grey lines). AG, Agua Rica; An, Antamina; BA, Bajo de La Alumbrera; BD, Bajo El Durazno; CC, Cero Casale; EI, El Indio; ET, El Teniente; LG, La Granja; LM, Lobo Marte; LP, Los Pelambres (+El Pachon); Ne, Navada; Pi, Pierina; Po, Portovelo; RB, Rio Blanco; To, Toromocho; Ya, Yanacocha.

does not seem to correspond with progressive subduction processes. Rather, ore deposits are concentrated at distinct regions that experienced pulses of intense metallogenic activity [1–3]. An example is the Miocene metallogenic belt in the central Andes that was formed during a relatively short period between 15 and 5 Ma [4], and is characterised by clusters of mineral deposits in northern Peru and in central Chile (Fig. 2).

In this paper we propose that a key factor for the occurrence of metallogenic episodes during progressive subduction is related to bathymetric heterogeneities within the subducting oceanic plate. Such heterogeneities are manifested by the subduction of topographic anomalies (e.g. seamounts, aseismic ridges, hotspot chains and oceanic plateaux), which is likely to result in a number of tectonic responses (e.g. [5–8]). For example, areas that involved the subduction of topographic anomalies are commonly characterised by flat subduction angles [9,10] and coincide with a gap in the spatial distribution of arc volcanism [11,12] and with high rates of tectonic erosion of the overriding plate [13–16]. This indicates that the whole dynamics of the subduction system is influenced by the subduction of topographic anomalies and it is therefore possible that metallogenic processes are also spatially and temporally linked with these areas of disturbed subduction (see also [17–20]).
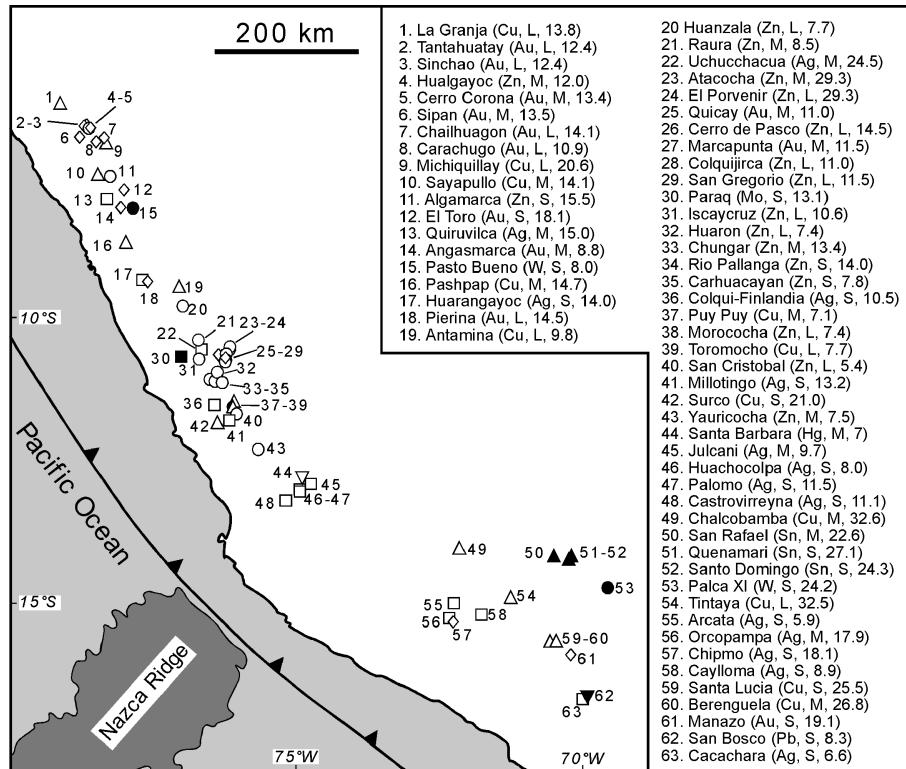
Fig. 2. The distribution of dated ore deposits in the Peruvian Andes. Symbols indicate zinc (open circles), copper (open triangles), silver (open squares), gold (open diamonds), molybdenum (filled squares), mercury (open inverted triangles), tin (filled triangles), tungsten (filled circles) and lead (filled inverted triangles). The bathymetric height of the Nazca Ridge (−4000 m contour) is also shown. The list of all deposits indicates the major metal in each deposit, the size of the deposit (L, large, M, medium, S, small), and the mineralisation age in Ma (for references see Online Supplementary Material Table S1).

Topographic anomalies within the subducting eastern margin of the Pacific Ocean (Fig. 1) include the Cocos Ridge [14], the Carnegie Ridge [21], the Nazca Ridge [15,16,22,23], the Iquique Ridge [24], and the Juan Fernandez Ridge [25]. The existence of an additional now-consumed topographic anomaly beneath northern Peru, the Inca Plateau, has been postulated by Gutscher et al. [24] based on seismic evidence and tectonic reconstructions (Fig. 1). Here we focus on the linear positive bathymetric anomaly of the Nazca Ridge, and to some extent, on the Inca Plateau (Figs. 1 and 2). Both topographic anomalies have started to subduct beneath the Peruvian Andes in the middle Miocene (15–11 Ma) [11,15,16,22–24,26]. An indirect link between the present-day distribution of ore deposits in Peru and subducting anomalies can be postulated based on the coincidence between the largest deposits and the volcanic gaps (Fig. 1). Here we show that the link becomes obvious when the spatiotemporal distribution of ore deposits is integrated in a plate reconstruction model. These results suggest that ridge subduction has possibly played a role in triggering the Miocene episode of magmatic–hydrothermal metallogenic activity in the Peruvian Andes.

## 2. Ore deposits in the Peruvian Andes

Research on ore deposits in the Peruvian Andes has been mainly focused on the nature and controls of individual deposits (e.g. [4,27]), whereas relatively little attention has been given to the spatial and temporal distribution of these deposits within the regional plate tectonic context. In order to investigate spatiotemporal relationships between metallogenic events and aseismic ridge subduction, we use available data

from 63 post-Oligocene sites of ore deposits in the Peruvian Andes (Fig. 2 and Online Supplementary Material Table S1). These deposits have been selected from a dataset comprising of 382 localities, using only those deposits that are reliably dated. Deposits older than 35 Ma have not been considered because they clearly cannot be related to the post-Miocene subduction of the Nazca Ridge or the Inca Plateau. Ages of

all the selected localities are considered to represent mineralisation ages. We have classified the deposits according to the major metal that is found at each locality and according to the relative size of each deposit (large, medium or small). The size is quantified based on the contained metal according to the following scheme (in tonnage): Cu and Zn deposits: large > 1,000,000, medium > 10,000, small < 10,000; Ag deposits: large > 100,000, medium > 1,000, small < 1000; Au deposits: large > 130, medium > 30, small < 30.

Several types of ore deposits of Miocene age are identified in Peru: (1) porphyry Cu–Au ± Mo deposits (e.g. La Granja, Antamina, Michiquillay, Tantahuatay); (2) high sulphidation epithermal Au–Ag deposits (e.g. Pierina, Sinchao, Quicay); (3) low sulphidation Au–Ag deposits (e.g. Arcata); and (4) Zn–Pb–Ag skarn, manto and chimney deposits (e.g. Cerro de Pasco, Huanzala, San Gregorio, Atacocha). Minor occurrences of Hg, W and Sn deposits are also found. Almost all of these deposits are associated with the intrusion of magmatic bodies. The overall temporal distribution of contained metals is summarised in Fig. 3 and shows an abrupt increase of metallogenic activity at ~15 Ma and a significantly intense metallogenic activity during the following ~8 Myr.

## 3. Kinematic reconstruction

The plate tectonic reconstruction (Fig. 4) takes into account the projected shapes of the subducted parts of the Nazca Ridge and the Inca Plateau, using similar methodology as previously described by Gutscher et al. [24] and Hampel [23]. Accordingly, the original geometries prior to subduction of the Nazca Ridge and the Inca Plateau are deduced from the shape of their conjugate features on the Pacific plate (the Tuamotu Plateau and the Marquesas Plateau, respectively). This is based on the assumption that each of the two pairs of topographic anomalies (the Nazca Ridge/Tuamotu Plateau and the Inca Plateau/Marquesas Plateau) formed simultaneously during symmetric sea-floor spreading at the East Pacific Rise [23,24,28]. Thus, for example, the shape and the length of the original Nazca Ridge in the reconstruction (Fig. 4) is the mirror image of the present-day Tuamotu Plateau.
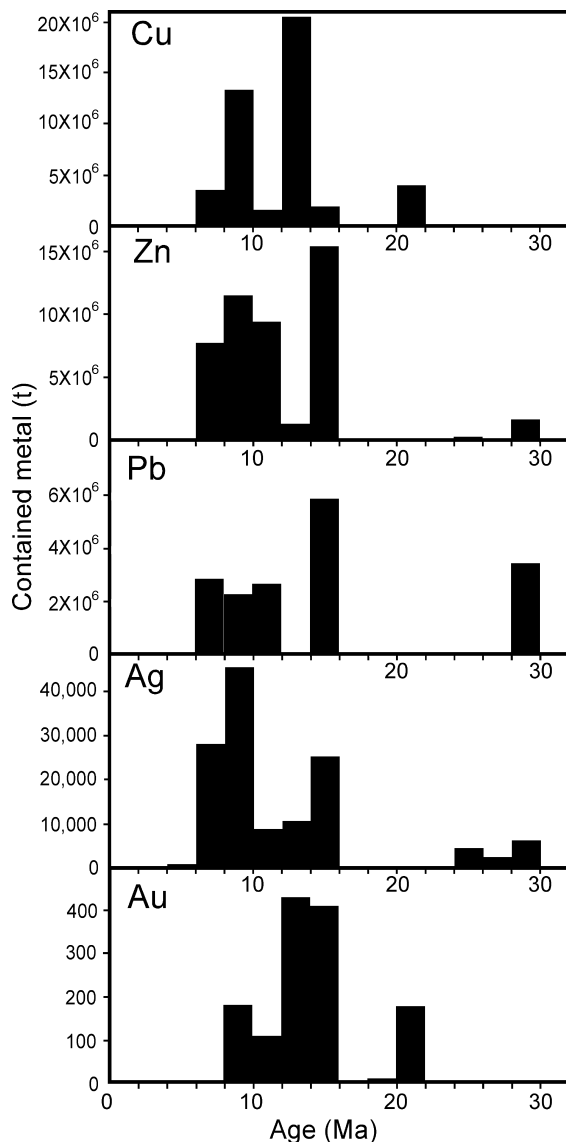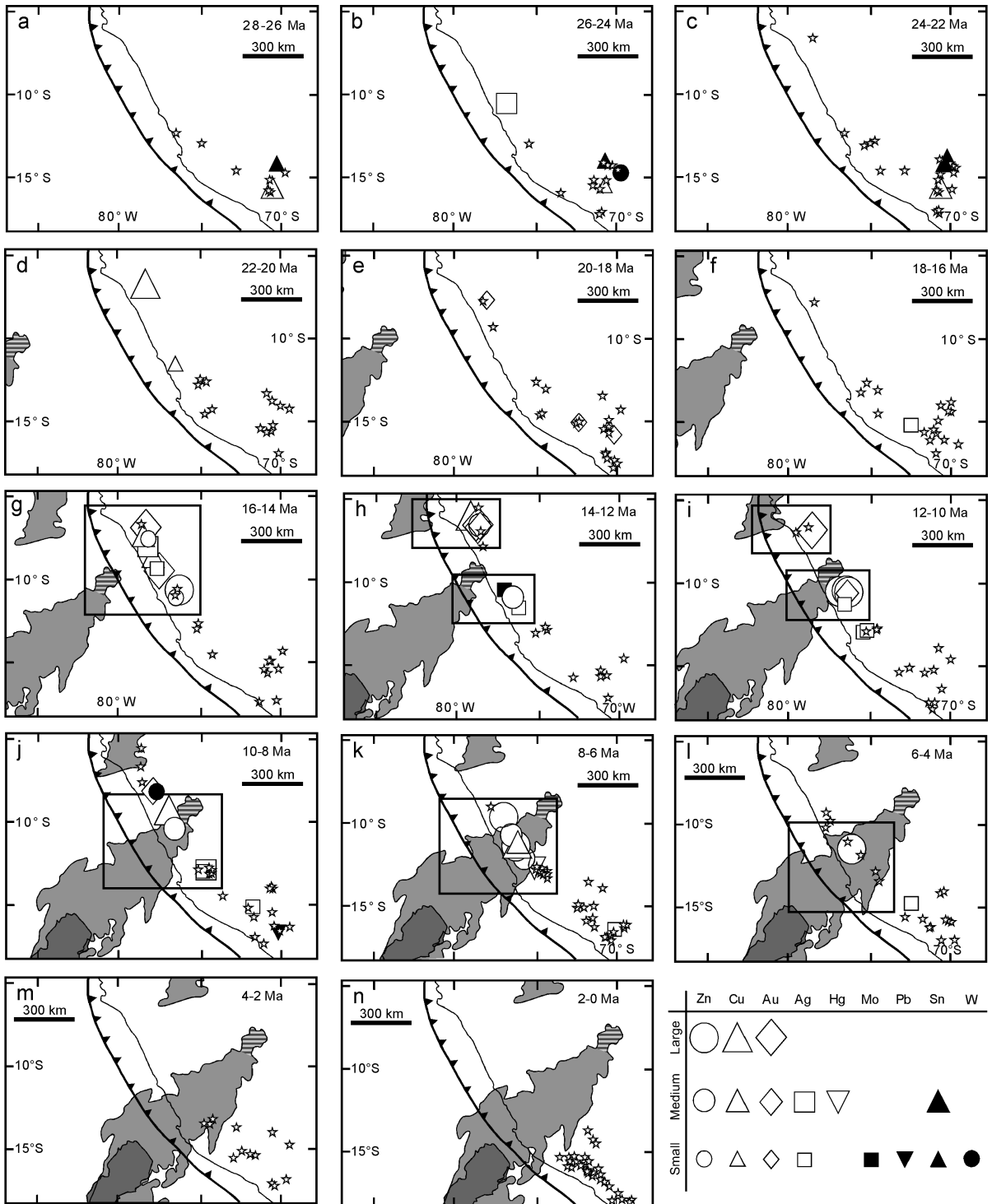


Fig. 3. Histograms showing the temporal distribution of ore deposits in Peru as indicated by the tonnage of contained metals (see Online Supplementary Material Table S1).

The determination of the relative convergence motion of the Nazca plate with respect to South America requires a plate circuit calculation. Our model is based on rotational parameters for the motions of the Nazca plate relative to the Pacific plate [29], the Pacific plate relative to Pacific Ocean hotspots [30], and South America relative to Atlantic and Indian Ocean hotspots [31]. This model assumes a fixed hotspot frame of reference. Therefore, some errors are introduced by the effect of relative motions between Indo-Atlantic and Pacific hotspot tracks (e.g. [32,33]). For example, according to the model of DiVenerea and Kent [32], during the Cenozoic, the Hawaiian hotspot moved in an average rate of 2–2.5 cm/yr relative to the Atlantic–Indian hotspots. Recent works by Tarduno et al. [34] and Steinberger et al. [35] suggest that since the Eocene, the rate of Hawaiian hotspot motion was considerably slower (ca. 1 cm/yr of southward motion), in contrast with very fast rates (4–5 cm/yr) that occurred prior to ~43 Ma. Relatively slow eastward to southwestward motions (≤1 cm/yr) have also been estimated for Indo-Atlantic hotspots [35]. Therefore, the assumption of fixed hotspots in our model may lead to maximum errors of 100–200 km during the period of 15–0 Ma. Considerable errors, however, could possibly exist in the earlier model of Somoza [36], in which the motion of the Nazca plate with respect to South America was calculated using a relatively cumbersome plate circuit (Nazca–Pacific–Antarctica–Africa–South America for the period of 40–16 Ma, and Nazca–Antarctica–Africa–South America for the period of 16–0 Ma).

The resulting rotational parameters are summarised in Table 1 and are used to develop the plate reconstruction shown in Fig. 4. In this reconstruction, the arrival of the Nazca Ridge at the subduction zone took place during oblique convergence at rates of 7–7.5 cm/yr.

The kinematic reconstruction in Fig. 4 shows that the arrival of the Nazca Ridge and the Inca Plateau at the subduction zone is temporally and spatially related

Table 1
Rotational parameters used in the kinematic reconstruction

| Age (Ma) | Latitude | Longitude | Rotation |
|---|---|---|---|
| *Nazca/Pacific [29]* | | | |
| 4.7 | 58.86 | − 89.43 | − 6.60 |
| 10.6 | 60.13 | − 89.76 | − 15.18 |
| 25.8 | 65.41 | − 92.00 | − 39.35 |
| | | | |
| *Pacific/hotspots [30]* | | | |
| 5.0 | − 56.50 | 104.90 | 4.70 |
| 10.83 | − 65.98 | 108.75 | 9.24 |
| 21.16 | − 70.45 | 111.79 | 17.43 |
| 25.0 | − 71.20 | 112.44 | 20.49 |
| | | | |
| *Nazca/hotspots (this study)* | | | |
| 4.7 | − 57.49 | 61.12 | 2.31 |
| 10.6 | − 48.28 | 76.39 | 6.44 |
| 25.8 | − 55.24 | 77.09 | 19.10 |
| | | | |
| *South America/hotspots [31]* | | | |
| 10.4 | 59.4 | − 45.8 | 1.80 |
| 20.5 | 65.8 | − 19.8 | 3.21 |
| 35.5 | 72.1 | 4.0 | 6.37 |

Latitudes and longitudes are in degrees (North and East positive). Rotation angles are in degrees (clockwise positive).

with a sudden burst in metallogenic activity at 15–13 Ma. According to this reconstruction, the tip of the Nazca Ridge began to interact with the subduction zone at ~15 Ma (Fig. 4g), somewhat earlier than previously suggested (11.2 Ma according to Hampel [23] or 13.5 Ma if we use Somoza's [36] rotational parameter in our reconstruction). The discrepancy is therefore derived from the slightly different rotational parameters used in our reconstruction, but also because of the ambiguous shape of the consumed part of the Nazca Ridge. According to Hampel [23], the northwesternmost tip of the Tuamotu Plateau did not have a counterpart mirror image on the Nazca plate because it was supposedly associated with younger (45–40 Ma) hotspot-related volcanism [37] that occurred ~600 km off the spreading ridge [38]. In

Fig. 4. Reconstruction of the subduction history of the Nazca Ridge and the Inca Plateau using recalculated plate motions (Table 1) and the lengths of the original Nazca Ridge and Inca Plateau (light grey) as deduced from the mirror shapes of the Tuamotu Plateau and the Marquesas Plateau on the Pacific plate [23,24]. Each reconstruction corresponds to the average age of the annotated time interval, and shows locations of ore deposits and volcanic centres that were active during that interval. The location of the non-subducted part of the Nazca Ridge is indicated by dark grey. The striped area indicates the mirror image of the northwestern tip of the Tuamotu Plateau for which the existence of a counterpart on the Nazca plate is controversial (see text). Subduction of the Nazca plate beneath South America is indicated by black triangles. Arc volcanism is indicated by stars. Boxes are shown to highlight areas of possible relationships between ore formation and ridge subduction.

this case, impingement of the Nazca Ridge took place only at 14–13 Ma (Fig. 4h). Based on geophysical data, however, it seems that the northwestern part of the Tuamotu Plateau represents a ca. 70-Ma crust that formed at the axis of the spreading ridge [39]. This view is supported by results of a recent seismic refraction profile [40], which indicate that the crust beneath the Tuamotu Plateau formed at or near the ridge axis. Therefore, in our reconstruction the mirror image of the tip of the Tuamotu Plateau (striped area in Fig. 4) was not omitted. We note, however, that this issue requires further geophysical and geochronological investigations.

The apparent increase in metallogenic activity at 15–13 Ma (Fig. 4g–h) is somewhat surprising. It suggests that impingement of the Nazca Ridge had an immediate metallogenic response. This is reflected by ore deposits that are located approximately 200 km from the subduction trench along a ~400-km long trench-parallel belt. The possibility that impingement of topographic anomalies at the subduction zone can trigger an immediate response at the overriding plate is further discussed in Section 5.2.

The reconstruction also shows that metallogenic activity roughly follows the Nazca ridge as it sweeps southwards along the coast of South America (Fig. 4i-l). This apparent link is valid for Cu, Au and Zn deposits, with a particularly large number of ore deposits concentrated on the overriding plate above the Nazca Ridge at 8–6 Ma (Fig. 4k). In contrast, Ag and Pb deposits are not spatially and temporally related to ridge subduction (e.g. Fig. 4j). Throughout the whole area, ore deposits younger than 4 Ma are not found, possibly because they have yet not been exposed by erosion.

A possible link is also recognised between ore deposits in northern Peru and the arrival of the Inca Plateau at the subduction system at ~13 Ma (Fig. 4h). This mineralisation included the large 12.4 Ma Au deposits in the Yanacocha district (Tantahuatay and Sinchao deposits). These deposits formed shortly after the arrival of the Inca Plateau at the subduction zone, indicating that metallogenic activity was triggered by the initial impingement of the topographic anomaly. In this region, there is no evidence for ore deposits younger than 10 Ma (Fig. 4j-n). This may be explained by the fact that at ca. 10 Ma the whole length of the Inca Plateau

(150–250 km) had already been consumed at the subduction zone.

## 4. Arc volcanism

The relations between ridge subduction and volcanism have been discussed by a number of authors (e.g. [11,12,41,42]). In these works, it has been recognised that flat subducting slabs, which are related to subduction of topographic anomalies, are commonly associated with occurrences of adakitic volcanism and a subsequent cessation of volcanism. Gutscher et al. [41] have explained the origin of adakitic magmas by partial melting of the subducting overthickened oceanic crust under hydrous conditions at depths of ca. 80 km. According to these authors, heating of the subducting slab is generated by a residual asthenospheric wedge, which is likely to cool after a few million years of ridge subduction, leading to the cessation of arc volcanism in a given area.

In the Peruvian Andes, a gap in the spatial distribution of present-day arc volcanism is well defined (Fig. 1). Here we have attempted to reconstruct the location of the active volcanic arc since 28 Ma (Fig. 4), using a dataset consisting of more than 400 dated samples of arc volcanism in Peru (see Supplementary Material Table S2). In the last 4 Myr, volcanism has been bounded by the subducting ridge and has been active only south of it. Interestingly, however, the current area of volcanic gap was subjected to relatively little volcanic activity also prior to ridge subduction (Fig. 4a-f).

The existence of volcanic gaps prior to 4 Ma is less defined. In general, volcanism tends to be more active to the south of the subducting ridge, but there are some active centres immediately above and to the north of the ridge. For example, a number of volcanic centres were active in central Peru at 6–4 Ma at the region above the subduction of the Nazca Ridge (Fig. 4l). Likewise, there was no clear volcanic gap during the subduction of the Inca Plateau (Fig. 4h-j).

As mentioned earlier, the development of ore deposits was intimately linked with magmatic processes. Nevertheless, the pattern of arc volcanism and ore deposits as shown in Fig. 4 suggests that volcanic activity did not play a major role during the formation of ore deposits. Rather, most of these

Table 2
The 10 largest young (<18 Ma) Cu porphyry deposits in South America

|   | Name | Location | Age (Ma) | Cu (Mt) | Reference | Associated topographic anomaly |
|---|------|----------|----------|---------|-----------|-------------------------------|
| 1 | El Teniente | Central Chile | 7.1–4.6 | 108.97 | [45] | Juan Fernandez |
| 2 | Rio Blanco | Central Chile | 5.4 | 50.00 | [45] | Juan Fernandez |
| 3 | Los Palembres and El Pachon | Central Chile | 10 | 26.22 | [45] | Juan Fernandez |
| 4 | La Granja | Northern Peru | 14.2–13.4 | 13.57 | See Supplementary Material Table S1 | Nazca and/or Inca |
| 5 | Antamina | Peru | 10.8–8.8 | 12.87 | See Supplementary Material Table S1 | Nazca |
| 6 | Agua Rica | Argentina | 6.3–4.9 | 7.37 | [45] | Juan Fernandez |
| 7 | Yanacocha (Tantahuatay + Sinchao) | Northern Peru | 12.8–12.0 | 6.23 | See Supplementary Material Table S1 | Inca |
| 8 | Bajo de la Alumbrera | Argentina | 8–7 | 4.06 | [45] | Juan Fernandez |
| 9 | Cerro Casale | Central Chile | 13.5 | 3.45 | [45] | Juan Fernandez |
| 10 | Toromocho | Peru | 8–7.4 | 2.68 | See Supplementary Material Table S1 | Nazca |

deposits were probably associated with plutonic processes.

## 5. Discussion

### 5.1. Coincidence of ridge subduction and ore formation

An apparent link between ridge subduction and metallogenic activity is suggested based on the high values of metal flux following the arrival of the Nazca ridge and the Inca Plateau at the subduction system (Fig. 3) and the apparent migration of the metallo-genic activity in tandem with the lateral movement of ridge subduction (Fig. 4). We now wish to demonstrate that a similar link may possibly exist at the scale of the whole Andean belt, where the distribution of the largest young (<18 Ma) ore deposits follows the pattern of subduction of topographic anomalies. In the scope of this discussion, we are unable to explain the distribution of older (>18 Ma) deposits, because there are no data on topographic anomalies that may have entered the subduction system prior to that time.

In the Central Andes, Mio–Pliocene ore deposits (<18 Ma) are scattered in a belt 2000 km long. However, the largest known Cu–Au and Au deposits of this age (Tables 2 and 3) define two clusters: one

Table 3
The 10 largest young (<18 Ma) Au deposits in South America

|   | Deposit name | Location | Age (Ma) | Au (t) | Reference | Associated topographic anomaly |
|---|--------------|----------|----------|--------|-----------|-------------------------------|
| 1 | Cerro Casale | Central Chile | 13.5 | 852 | [45] | Juan Fernandez |
| 2 | Bajo de la Alumbrera | Argentina | 8–7 | 523 | [45] | Juan Fernandez |
| 3 | Nevada | Central Chile | ~11 | 434 | [45] | Juan Fernandez |
| 4 | El Indio–Tambo | Central Chile | 11–9 | 413 | [45] | Juan Fernandez |
| 5 | Agua Rica | Argentina | 6.3–4.9 | 291 | [45] | Juan Fernandez |
| 6 | Yanacocha (Tantahuatay + Sinchao) | Northern Peru | 12.8–12.0 | 289 | See Supplementary Material Table S1 | Inca |
| 7 | Portovelo | Ecuador | ~15 | 242 | [56] | Inca |
| 8 | Bajo de Durzano | Argentina | 8.0 | 225 | [45] | Juan Fernandez |
| 9 | Pierina | Peru | 14.9–14.1 | 225 | See Supplementary Material Table S1 | Nazca |
| 10 | Lobo-Marte | Central Chile | 13.0 | 222 | [45] | Juan Fernandez |

in central-northern Peru and the other in central Chile (Fig. 1). As noted before, the spatial distribution of these giant deposits coincides with gaps in the spatial distribution of active volcanism and with the location of two major segments of flat subduction (the Peru flat slab and the Central Chile flat slab [9]).

In Fig. 5, we have used the reconstruction of the Juan Fernandez hotspot chain [43] to predict the lateral migration of the locus of aseismic ridge subduction in central Chile. The whole region has been subjected to relatively flat subduction in the last 18 Ma, which was accompanied by the cessation of arc and back-arc volcanism [44]. The largest ore deposits in this region
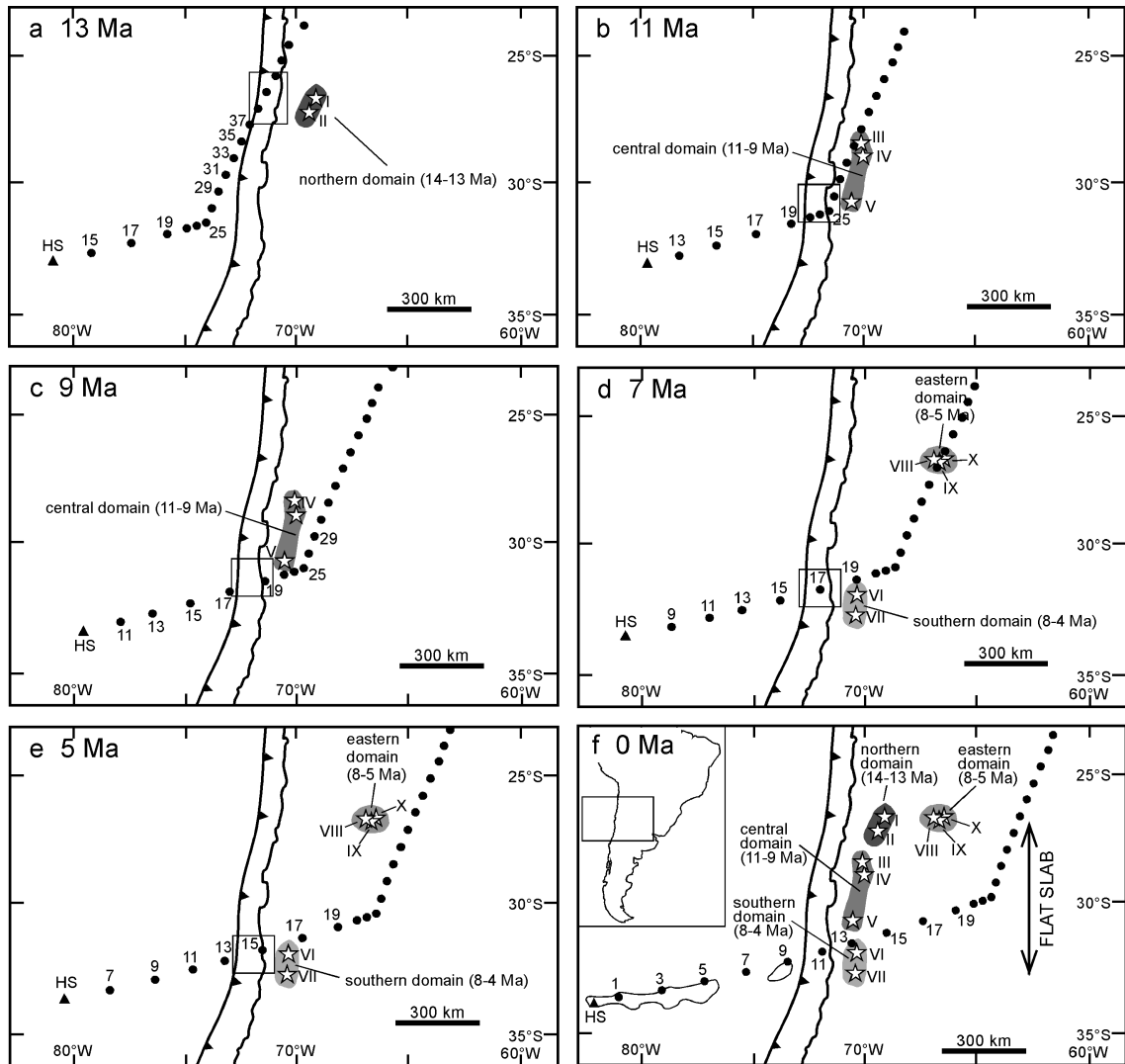


Fig. 5. Reconstruction of the Juan Fernandez hotspot chain based on the rotational parameters shown in Table 1 and the predicted path of the Juan Fernandez hotspot chain (after [43]). Locations of the largest Cu and Cu–Au ore deposits in Chile are indicated by stars (see Tables 2 and 3). The metallogenic belt is divided here into four domains that coincide with the area of flat subduction. Boxes highlight areas where the hotspot chain meets the subduction zone. Note that at all stages excluding 9 Ma, these areas roughly coincide with the locus of metallogenic activity. Ore deposits are: I, Lobo Marte; II, Cerro Casale; III, Nevada; IV, El Indio; V, Los Pelambres and El Pachon, VI, Rio Blanco; VII, El Teniente; VIII, Bajo de la Alumbrera; IX, Bajo el Durazno; X, Agua Rica. Numbers indicate ages of predicted hotspot volcanism. Active hotspot is indicated by a triangle (HS).

(Tables 2 and 3) can be divided into four metallogenic domains (Fig. 5f). Across the northern, central and southern domains, there is an overall southward younging of metallogenic activity. This trend roughly follows the migration of aseismic ridge subduction (Fig. 5a-e). The 8–5-Ma ore deposits in the eastern domain are located in an anomalous position relative to the rest of the deposits, but seems to coincide with the location at depth of the aseismic ridge approximately 400 km from the subduction zone (Fig. 5d).

None of the large ore deposits listed in Tables 2 and 3 (i.e. ore deposits younger than 18 Ma) are located in the area where subduction of the Iquique Ridge takes place in northern Chile (Fig. 1). The lack of young metallogenic fields associated with the subduction of the Iquique Ridge is particularly interesting because this province in northern Chile was remarkably fertile during the Eocene–Oligocene (41–31 Ma), hosting some of the largest ore deposits in the Andes (e.g. Chuquicamata, La Escondida, Rosario and El Salvador) [45]. We do not know what triggered this older mineralisation. However, if we reconstruct the shape and length of the Iquique Ridge using the kinematic parameters in Table 1 (Fig. 6), we are able to explain why younger deposits related to the subduction of the Iquique ridge are missing. Such reconstruction, which is based on the mirror shape of the Austral Plateau [24], shows that the ridge has started to be subducted very recently (<2 Ma). Therefore, any deposits that might have been produced are unlikely to be exposed at the surface. Fig. 1 indicates that a narrow volcanic gap related to the Iquique Ridge has already been developed. Another possibility is that ore deposits related to the Iquique Ridge have not formed due to the depletion of metal sources following the first mineralisation event.

There are, of course, several ore deposits in the Central Andes that cannot be linked with ridge subduction, as for example, the ~14-Ma Kori Kollo gold deposit in Bolivia (ca. 160 tonnes gold [45]), which is located about 1000 km southeast of the Nazca Ridge. It is therefore stressed that ridge subduction is not a necessary factor for the formation of large subduction-related ore deposits. It may, however, trigger favoured geodynamic conditions for giant magmatic–hydrothermal ore formation.

The apparent link between the impingement of topographic anomalies at the subduction zone and
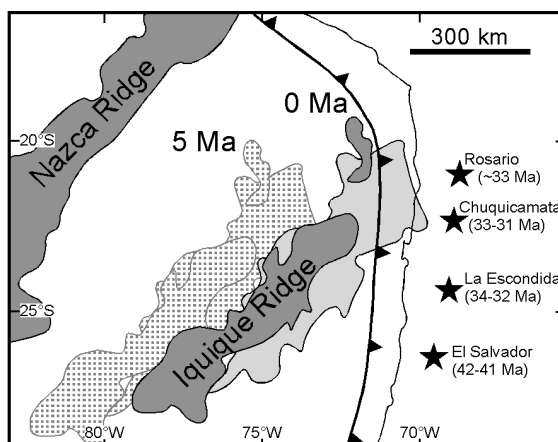


Fig. 6. Reconstruction of the shape and length of the Iquique Ridge, showing that the arrival of this topographic anomaly at the subduction system has occurred very recently. The reconstruction is based on the geometry of the anomaly's counterpart west of the East Pacific Rise (the Austral Plateau) [24] and the kinematics of the Nazca plate with respect to South America (Table 1). The present-day locations of the Iquique Ridge and the Nazca Ridge are indicated by dark grey, whereas the predicted shape of the Iquique Ridge as inferred from the mirror shape of the Austral Plateau is indicated by light grey. The predicted location of the Iquique Ridge at 5 Ma (including the small consumed part of the anomaly) is shown in the dotted area. Also shown are locations of giant ore deposits in northern Chile. All these deposits are of Eocene–Oligocene age and are thus not related to the subduction of the Iquique Ridge.

anomalous metal flux in the overriding plate may provide an important insight into the geodynamic environment that exists during the formation of large subduction-related ore deposits. It has been already suggested that the occurrence of giant porphyry-related ore deposits are related to abrupt tectonic changes in the subduction zone, such as the reversal of arc polarity [46] or the flattening of the subducting slab [20,47]. In the Central Andes, it has also been noted that magmatic activity associated with the formation of porphyry-related ore deposits was usually the last intrusive event in a given area, thus representing the termination of a magmatic cycle [48]. Such changes can possibly be associated with the formation of volcanic gaps following ridge subduction. We further discuss these ideas in the following section.

## 5.2. Geodynamic implications

A schematic illustration of magmatic–hydrothermal processes that occur in a suprasubduction envir-

onment is shown in Fig. 7a [48]. According to this model, fertile calc-alkaline magmas are generated in the MASH zone—a zone of melting, assimilation, storage and homogenisation [49]. This zone is a relatively narrow band in the lowermost crust or mantle–crust transition, where mixing between mantle-derived melts and assimilated crustal rocks takes place. Magmatic processes in the MASH zone are likely to occur during periods of stable subduction, in which the slab dips beneath the arc at a constant angle and constant velocity [48]. This process may increase the potential for metallogenic fertility, but in order to give rise to ore deposits, it is required that exsolution of the metalliferous and sulphur-rich hydrothermal fluids from the calc-alkaline magma takes place. Ore minerals will eventually be deposited in response to cooling of the wall-rocks, fluid phase separation or mixing with external fluids [48]. In the next paragraphs we speculate that this final stage of ore body formation is possibly triggered by the tectonic changes associated with ridge subduction.

As mentioned before, a large number of ore deposits in northern Peru developed immediately upon impingement of the edge of the aseismic ridge into the subduction zone (Fig. 4g). We note that this surprising observation could possibly be associated with errors in our reconstruction model (e.g. imprecise rotational parameters and geochronological ages, inaccurate reconstruction of the shape of the topographic anomalies, or eastward movement of the subduction zone due to shortening of the overriding plate in the Andes). However, if our model is correct, then we must assume that an important factor for ore deposit formation is the change in the state of stress in the crust, which is triggered by the initial impingement of topographic anomalies into the subduction zone. It has already been discussed (e.g. [6]) that impingement of aseismic ridges would give rise to increased coupling between the two plates that would lead to enhanced seismicity and crustal deformation. Faults associated with this deformation could then mobilize fertile magmas in the MASH zone to travel towards shallower depths. The exsolution of fluids at shallow levels can ultimately lead to final metal concentration. Crustal deformation is also likely to increase permeability and to facilitate fluid pathways at shallow crust and melt pathways from depth [50], thus

promoting the deposition of ore minerals in fracture-related structures (e.g. manto and veins). Metal fertility, according to this model, was already latent in the crust, as predicted also from the MASH model [48] (Fig. 7a).

Analogue modelling [51] has shown that impingement of a topographic anomaly into the overriding plate is likely to produce a deformational pattern associated with folding and thrusting immediately in front of the ridge and fanning pattern of strike–slip faulting on either side of the ridge. Thus, the ore deposits in Fig. 4g that occur immediately in front of the ridge could be related to shortening deformation, whilst ore deposits at the northwest and southeast extremities, and also the ore deposits in Fig. 4h, could possibly be related to the fanning of strike–slip deformation. This suggested deformational pattern can be examined in northern Peru by further structural investigations.

An additional explanation for ore deposit formation can be attributed to the flattening of the subducting slab following ridge subduction [20]. This explanation, however, cannot account for those deposits that formed immediately upon the initial impingement because flat subduction is likely to develop only after considerable subduction of the relatively buoyant anomaly (e.g. [10]). The cluster of deposits in central Peru at 8–6 Ma (Fig. 4k) could possibly be associated with flattening of the subducting slab. As shown in Fig. 7b, a change in the dip of the slab is likely to interfere with the evolution of the magmatic arc, leading to cooling of the asthenospheric wedge and the termination of a given magmatic cycle. Arc volcanism is therefore likely to shut down or to be shifted to a different locus. There are several possibilities as to the reason why ore deposits will form at this stage: (1) It is possible that volcanic eruptions act as a negative factor in ore body formation because of the potential metal loss that occurs when sulphur-rich volatiles are released to the atmosphere [52]. Thus, the cessation of arc volcanism may actually help to preserve metals in the magmatic reservoir, promoting rock/magma interactions and the deposition of ore deposits. (2) The tectonic change associated with slab flattening is likely to lead to the termination of a magmatic cycle, thus promoting the deposition of ore minerals in porphyry-type rocks. (3) It is possible that metalliferous fluids are derived from melting of
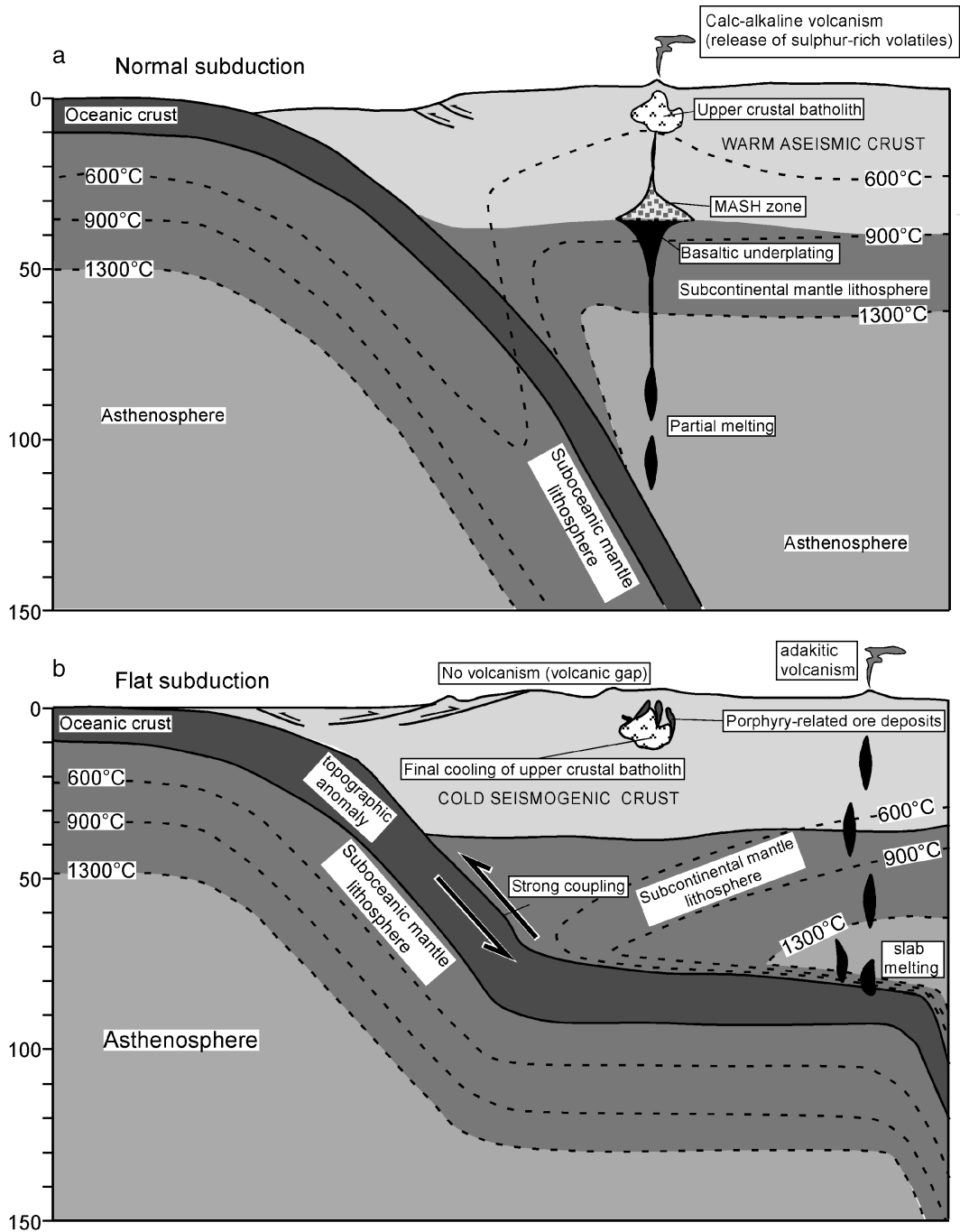
Fig. 7. Cartoons showing magmatic–hydrothermal processes in suprasubduction setting and the tectonic changes that occur after the subduction of a relatively buoyant aseismic ridge (partly modified after [9,41,48,55]). (a) Subduction of normal oceanic lithosphere beneath potentially fertile continental crust. (b) Shallow subduction following the arrival of an aseismic ridge at the subduction zone and associated tectonic features (cessation of volcanism in the magmatic arc, intense seismicity, possible production of adakitic magmas from slab melting, and cooling of porphyry-type magmas during late crystallisation stages of upper crustal batholiths).

the subducting slab, as indicated by the formation of adakitic magmas (e.g. in Ecuador and Chile [41,42]). Our results, however, suggest that the development of flat subduction was not the primary mechanism that controlled ore deposit formation (c.f. [20]), as attested, for example, by the lack of young (<10 Ma) ore deposits related to the Inca Plateau regardless of the pronounced flat subduction in this region.

## 6. Conclusions

This study shows a spatial and temporal link between ridge subduction and ore body formation in the Peruvian Andes, with high metal fluxes concentrated in zones of ridge subduction during the subduction of the Nazca Ridge and the Inca Plateau. Furthermore, the subduction of the Juan Fernandez Ridge in Central Chile possibly accounts for the intense metallogenic activity in this region since the middle Miocene and to the lateral changes in the spatio-temporal distribution of the metallogenic domains in the area. Our reconstruction approach has the potential to be applied to other areas of ridge subduction, in which there is mature datasets on ore deposits, and may be expanded to include palaeo-subduction systems. Thus, the recognition of tectonic features that are related to subduction of topographic anomalies can possibly provide insights into predictive mineral discovery by enhancing our ability to predict the position of large mineral deposits in other modern and ancient orogens.

## Acknowledgements

## Appendix A. Supplementary data

Supplementary data associated with this article can be found, in the online version, at doi:10.1016/j.epsl.2005.08.003.

## References

[1] R.H. Sillitoe, Tectonic segmentation of the Andes: implications for magmatism and metallogeny, Nature 250 (1974) 542–545.

[2] R.H. Sillitoe, Epochs of intrusion-related copper mineralization in the Andes, J. S. Am. Earth Sci. 1 (1988) 89–108.

[3] U. Petersen, Geological framework of Andean mineral resources, in: G.E. Ericksen, M.T.C. Pinochet, J.A. Reinemund (Eds.), Geology of the Andes and Its Relation to Hydrocarbon and Mineral Resources 11, Circum-Pacific Council for Energy and Mineral Resources Earth Science Series, Houston, 1990, pp. 213–232.

[4] D.C. Noble, E.H. McKee, The Miocene metallogenic belt of central and northern Peru, in: B.J. Skinner (Ed.), Geology and Ore Deposits of the Central Andes 7, Society of Economic Geologists Special Publication, 1999, pp. 155–193.

[5] W.Y. Chung, H. Kanamori, A mechanical model for plate deformation associated with aseismic ridge subduction in the New Hebrides Arc, Tectonophysics 50 (1978) 29–40.

[6] L.V. LeFevre, K.C. McNally, Stress distribution and subduction of aseismic ridges in the Middle America subduction zone, J. Geophys. Res. 90 (1985) 4495–4510.

[7] S.E. Lallemand, J. Malavieille, S. Calassou, Effects of oceanic ridge subduction on accretionary wedges: experimental modeling and marine observations, Tectonics 11 (1992) 1301–1313.

[8] M. Cloos, Lithospheric buoyancy and collisional orogenesis: subduction of oceanic plateaus, continental margins, island arcs, spreading ridges, and seamounts, Geol. Soc. Amer. Bull. 105 (1993) 715–737.

[9] M.-A. Gutscher, W. Spakman, H. Bijwaard, E.R. Engdahl, Geodynamics of flat subduction: seismicity and tomographic constraints from the Andean margin, Tectonics 19 (2000) 814–833.

[10] J. van Hunen, A.P. van der Berg, N.J. Vlaar, On the role of subducting oceanic plateaus in the development of shallow flat subduction, Tectonophysics 352 (2002) 317–333.

[11] A. Nur, Z. Ben-Avraham, Volcanic gaps and the consumption of aseismic ridges in South America, in: L.D. Kulm, J. Dymond, E.J. Dasch, D.M. Hussong, R. Roderick (Eds.), Nazca Plate: Crustal Formation and Andean Convergence 154, Geological Society of America Memoir, 1981, pp. 729–740.

[12] S. McGeary, A. Nur, Z. Ben-Avraham, Spatial gaps in arc volcanism: the effect of collision or subduction of oceanic plateaus, Tectonophysics 119 (1985) 195–221.

[13] J.Y. Collot, M.A. Fisher, Formation of forearc basins by collisions between seamounts and accretionary wedges: an example from the New Hebrides subduction zone, Geology 17 (1989) 930–933.

[14] C.R. Ranero, R. von Huene, Subduction erosion along the Middle America convergent margin, Nature 404 (2000) 748–752.

[15] P.D. Clift, I. Pecher, N. Kukowski, A. Hampel, Tectonic erosion of the Peruvian forearc, Lima Basin, by subduction and

Nazca Ridge collision, Tectonics 22 (2003) 1023, doi:10.1029/2002TC001386.

[16] A. Hampel, N. Kukowski, J. Bialas, C. Huebscher, R. Heinbockel, Ridge subduction at an erosive margin: collision zone of the Nazca Ridge in southern Peru, J. Geophys. Res. 109 (2004), doi:10.1029/2003JB002593.

[17] M.A. Skewes, C.R. Stern, Tectonic trigger for the formation of late Miocene Cu-rich breccia pipes in the Andes of central Chile, Geology 22 (1994) 551–554.

[18] P.J. Haeussler, D.C. Bradley, R.J. Goldfarb, L.W. Snee, C.D. Taylor, Link between ridge subduction and gold mineralization in Southern Alaska, Geology 23 (1995) 995–998.

[19] S.M. Kay, C. Mpodozis, B. Coira, Neogene magmatism, tectonism, and mineral deposits of the Central Andes (22° to 33°S latitude), in: B.J. Skinner (Ed.), Geology and Ore Deposits of the Central Andes 7, Society of Economic Geologists Special Publication, 1999, pp. 27–59.

[20] S.M. Kay, C. Mpodozis, Central Andean ore deposits linked to evolving shallow subduction systems and thickening crust, GSA Today 11 (2001) 4–9.

[21] P. Lonsdale, Ecuadorian subduction system, AAPG Bull. 62 (1978) 2454–2477.

[22] R. von Huene, I.A. Pecher, M.A. Gutscher, Development of the accretionary prism along Peru and material flux after subduction of Nazca Ridge, Tectonics 15 (1996) 19–33.

[23] A. Hampel, The migration history of the Nazca Ridge along the Peruvian active margin: a re-evaluation, Earth Planet. Sci. Lett. 203 (2002) 665–679.

[24] M.A. Gutscher, J.L. Olivet, D. Aslanian, J.P. Eissen, R. Maury, The "lost Inca Plateau": cause of flat subduction beneath Peru? Earth Planet. Sci. Lett. 171 (1999) 335–341.

[25] R. von Huene, J. Corvalán, E.R. Flueh, K. Hinz, J. Korstgard, C.R. Ranero, W. Weinrebe, CONDOR Scientists, tectonic control on the subducting Juan Fernandez Ridge on the Andean margin near Valparaiso, Chile, Tectonics 16 (1997) 474–488.

[26] R.A. Hagen, R. Moberly, Tectonic effects of a subducting aseismic ridge: the subduction of the Nazca Ridge at the Peru Trench, Mar. Geophys. Res. 16 (1994) 145–161.

[27] B.J. Skinner (Ed.), A special issue devoted to the mineral deposits of Peru, Economic Geology, 1990, 1287–1685 pp.

[28] R.H. Pilger, Plate reconstructions, aseismic ridges, and low-angle subduction beneath the Andes, Geol. Soc. Amer. Bull. 92 (1981) 448–456.

[29] C.L. Mayes, L.A. Lawver, D.T. Sandwell, Tectonic history and new isochron chart of the South Pacific, J. Geophys. Res. 95 (1990) 8543–8567.

[30] C.A. Raymond, J.M. Stock, S. Cande, Fast Paleogene motion of the Pacific hotspots from revised global plate circuit constraints, Geophys. Monogr. 121 (2000) 359–375.

[31] R.D. Müller, J.-Y. Royer, L.A. Lawver, Revised plate motions relative to the hotspots from combined Atlantic and Indian Ocean hotspot tracks, Geology 21 (1993) 275–278.

[32] V. DiVenerea, D.V. Kent, Are the Pacific and Indo-Atlantic hotspots fixed? Testing the plate circuit through Antarctica, Earth Planet. Sci. Lett. 170 (1999) 105–117.

[33] C. O'Neill, D. Müller, B. Steinberger, On the uncertainties in hot spot reconstructions and the significance of moving hot spot reference frames, Geochem. Geophys. Geosyst. 6 (2005) Q04003, doi:10.1029/2004GC000784.

[34] J.A. Tarduno, R.A. Duncan, D.W. Scholl, R.D. Cottrell, B. Steinberger, T. Thordarson, B.C. Kerr, C.R. Neal, F.A. Frey, M. Torii, C. Carvallo, The Emperor Seamounts: southward motion of the Hawaiian hotspot plume in earth's mantle, Science 301 (2003) 1064–1069.

[35] B. Steinberger, R. Sutherland, R.J. O'Connell, Prediction of Emperor–Hawaii seamount locations from a revised model of global plate motion and mantle flow, Nature 430 (2004) 167–173.

[36] R. Somoza, Updated Nazca (Farallon)–South America relative motions during the last 40 My; implications for mountain building in the Central Andean region, J. S. Am. Earth Sci. 11 (1998) 211–215.

[37] S.O. Schlanger, M.O. Garcia, B.H. Keating, J.J. Naughton, W.W. Sager, J.A. Haggerty, J.A. Philipotts, Geology and geochronology of the line islands, J. Geophys. Res. 89 (1984) 11261–11272.

[38] G. Ito, M. McNutt, R.L. Gibson, Crustal structure of the Tuamotu Plateau, 15°S, and implications for its origin, J. Geophys. Res. 100 (1995) 8097–8114.

[39] J. Talandier, E.A. Okal, Crustal structure in the Society and Tuamotu Islands, French Polynesia, Geophys. J. R. Astron. Soc. 88 (1987) 499–528.

[40] M. Patriat, F. Klingelhoefer, D. Aslanian, I. Contrucci, M.-A. Gutscher, J. Talandier, F. Avedik, J. Francheteau, W. Weigel, Deep crustal structure of the Tuamotu Plateau and Tahiti (French Polynesia) based on seismic refraction data, Geophys. Res. Lett. 29 (2002), doi:10.1029/2001GL013913.

[41] M.-A. Gutscher, R. Maury, J.-P. Eissen, E. Bourdon, Can slab melting be caused by flat subduction? Geology 28 (2000) 535–538.

[42] B. Beate, M. Monzier, R. Spikings, J. Cotten, J. Silva, E. Bourdon, J.-P. Eissen, Mio–Pliocene adakite generation related to flat subduction in southern Ecuador: the Quimsacocha volcanic center, Earth Planet. Sci. Lett. 192 (2001) 561–570.

[43] G.A. Yáñez, C.R. Ranero, R. von Huene, J. Díaz, Magnetic anomaly interpretation across the southern central Andes (32°S–34°S): the role of the Juan Fernandez Ridge in the late Tertiary evolution of the margin, J. Geophys. Res. 106 (2001) 6325–6345.

[44] S.M. Kay, V. Maksaev, R. Moscoso, C. Mpodozis, C. Nasi, C.E. Gordillo, Tertiary Andean magmatism in Chile and Argentina between 28°S and 33°S: correlation of magmatic chemistry with a changing Benioff zone, J. S. Am. Earth Sci. 1 (1988) 21–39.

[45] F.E. Mutschler, S. Ludington, A.A. Bookstrom, Giant porphyry-related metal camps of the world—a database, USGS Open File Rep. 99-556, 1999. http://geopubs.wr.usgs.gov/open-file/of99-556/.

[46] M. Solomon, Subduction, arc reversal, and the origin of porphyry copper–gold deposits in island arcs, Geology 18 (1990) 630–633.

[47] R. Kerrich, R. Goldfarb, D. Groves, S. Garwin, The geodynamics of world-class gold deposits; characteristics, space-

time distribution, and origins, Rev. Econ. Geol. 13 (2000) 501–551.

[48] J.P. Richards, Tectono-magmatic precursors for porphyry Cu-(Mo–Au) deposit formation, Econ. Geol. 98 (2003) 1515–1533.

[49] W. Hildreth, S. Moorbath, Crustal contributions to arc magmatism in the Andes of Central Chile, Contrib. Mineral. Petrol. 98 (1988) 455–489.

[50] S.F. Cox, J. Braun, M.A. Knackstedt, Principles of structural control on permeability and fluid flow in hydrothermal systems, Rev. Econ. Geol. 14 (2001) 1–24.

[51] W.P. Schellart, G.S. Lister, M.W. Jessell, Analogue modeling of arc and backarc deformation in the New Hebrides Arc and North Fiji Basin, Geology 30 (2002) 311–314.

[52] J.D. Pasteris, Mount Pinatubo volcano and "negative" porphyry copper deposits, Geology 24 (1996) 1075–1078.

[53] W.H.F. Smith, D.T. Sandwell, Global seafloor topography from satellite altimetry and ship depth soundings, Science 277 (1997) 1957–1962.

[54] C. DeMets, R.G. Gordon, D.F. Argus, S. Stein, Current plate motions, Geophys. J. Int. 101 (1990) 425–478.

[55] E.P. Nelson, Suprasubduction mineralization: metallo-tectonic terranes of the southernmost Andes, Geophys. Monogr. 96 (1996) 315–330.

[56] M. Billa, D. Cassard, A.L.W. Lips, V. Bouchot, B. Tourliere, G. Stein, L. Guillou-Frottier, Predicting gold-rich epithermal and porphyry systems in the central Andes with a continental-scale metallogenic GIS, Ore Geol. Rev. 25 (2004) 39–67.